LEARNING THE FUNDAMENTALS OF KINETICS AND REACTION ENGINEERING

With the Catalytic Oxidation of Methane

Viktor J. Cybulskis, Andrew D. Smeltz, Yury Zvinevich, Rajamani Gounder, W. Nicholas Delgass, and Fabio H. Ribeiro
Purdue University • Lafayette, IN 47907-2100 USA

The principles of chemical kinetics and reaction engineering are part of the core disciplines within chemical engineering and among the most desired skills sought by engineering employers.[1] Chemical reactions often do not occur spontaneously at reasonable process temperatures and require catalysts to increase their rates and to selectively influence reaction pathways to desired products. Catalytic materials are ubiquitous in the chemical and refining industries and will be used in technologies that shape the future of clean energy and chemical production.[2] In a heterogeneously catalyzed process, the chemical reaction occurs at a fluid-solid interface through a sequence of elementary steps involving molecules and reaction intermediates adsorbed onto active sites on the catalyst surface.[3] The kinetic details of these elementary steps contain fundamental information about the surface chemistry involved in the reaction and can provide insight into the underlying reaction mechanism. Furthermore, chemical engineers apply knowledge about how process variables such as temperature, reactant and product concentrations and flow rates, catalyst surface area, and active site density can influence reaction rates in order to optimize existing chemical processes or to design improved catalytic materials.

There are many examples of laboratory reactors that are used for chemical engineering instruction in kinetics,[4] reaction engineering,[5] and heterogeneous catalysis,[6,7] yet few have the capability to perform simplified experiments that demonstrate multiple aspects of chemical reaction engineering such as chemical kinetics, reactor design, and catalysis. The laboratory unit that we have designed provides chemical engineering students with a hands-on learning tool to supplement their classroom curriculum in chemical kinetics and reaction engineering. Our instructional reactor unit is mobile, is constructed with inherent safety features, and is versatile in its ability to perform multiple types of experiments with precise measurements, as described in the next section.

The catalytic oxidation of methane ($CH_4 + 2O_2 \rightarrow CO_2 + 2H_2O$) by a supported metal catalyst—an industrially relevant process—is used as a model reaction for this experiment. Methane is considered to be the most eco-friendly fossil fuel because it has the highest hydrogen-to-carbon ratio of

***Viktor J. Cybulskis**, P.E., is a fifth-year Ph.D. candidate in chemical engineering at Purdue University and received his B.S. in chemical engineering from Purdue University. His research interests include studies in heterogeneous catalysis and the development of operando and transient spectroscopic techniques. He is a licensed professional engineer in the state of Indiana.*

***Andrew D. Smeltz** is a principal investigator at United Technologies Research Center. He received his Ph.D. in chemical engineering from Purdue University and his B.S. in chemical engineering from Ohio University. His responsibilities include chemical process design and systems engineering, materials science and engineering, and the development of electrical energy storage technologies.*

***Yury Zvinevich** is the director of Instrumentation for the School of Chemical Engineering at Purdue University. He received his Ph.D. in optics and laser physics from the Institute of Physics in Belarus.*

***Rajamani Gounder** is an assistant professor in the School of Chemical Engineering at Purdue University. He received his Ph.D. in chemical engineering from the University of California, Berkeley, and his B.S. in chemical engineering from the University of Wisconsin. His research interests include studies in heterogeneous catalysis and the synthesis of zeolites and molecular sieves.*

***W. Nicholas Delgass** is the Maxine Spencer Nichols Emeritus Professor of Chemical Engineering at Purdue University. He received his Ph.D. and M.S. degrees in chemical engineering from Stanford University and his B.S. in chemical engineering from the University of Michigan. His research interests include studies in heterogeneous catalysis and the development of steady state and transient spectroscopic techniques.*

***Fabio H. Ribeiro** is the R. Norris and Eleanor Shreve Professor of Chemical Engineering at Purdue University. He received his Ph.D. and M.S. degrees in chemical engineering from Stanford University along with an M.S. in chemistry and a B.S. in chemical engineering from the Instituto Militar de Engenharia in Brazil. His research interests include the kinetics of heterogeneous catalytic processes and the development of steady state and transient spectroscopic techniques.*

TABLE 1
Experimental capabilities for catalytic reaction unit

Topic	Experiments
Chemical Kinetics	Determine rates of reaction
	Determine reaction orders
	Determine temperature dependence (activation energy)
	Examine inhibition effects by reaction products
Reactor Design	Measure kinetics in various reactor types (batch, PFR, CSTR)
	Study heat and mass transfer effects in heterogeneous catalysts

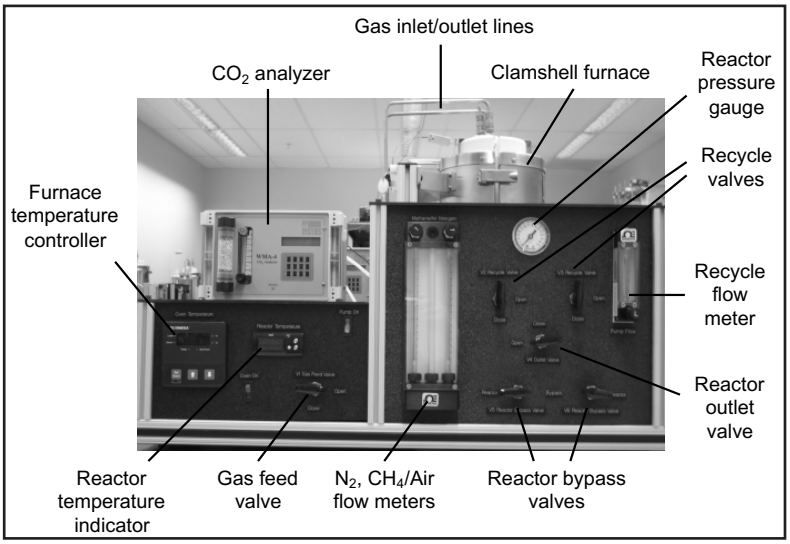

Figure 1. *The self-contained laboratory catalytic reaction unit.*

any hydrocarbon molecule (H/C = 4) and typically contains low levels of nitrogen and sulfur, which minimizes the effect of impurities on reactor performance.[8] Furthermore, when methane is oxidized at low temperatures (<550 K) in a catalytic process, lower levels of NO_x atmospheric pollutants are generated than in higher-temperature thermal combustion processes. Previous experimental studies have shown that supported Pd catalysts are the most practical materials for catalytic methane combustion due to the high turnover rate (TOR) per metal surface area.[9,10]

APPARATUS AND METHODS

The experimental apparatus is a self-contained catalytic reaction unit (Figure 1) that can be used to perform a variety of experiments (Table 1), each of which can be conducted during a two-hour laboratory session. These experiments provide students with the ability to gain experience with different types of chemical reactors, and to observe the effects of product inhibition and intrapellet mass transfer limitations, which are two common artifacts in the measurement of kinetic data.

TABLE 2
Equipment parts list and cost estimate per experimental unit*

Item	Quantity	Est. Unit Cost / USD	Total Cost / USD
Swagelok SS-41GXS2 1/8" 3-way ball valve	6	$90.00	$540.00
Swagelok SS-4L 1/4" metering valve	1	$100.00	$100.00
Swagelok SS-RL3S4 1/4" low pressure proportional relief valve	1	$180.00	$180.00
Swagelok SS-200-3 1/8" union tee	9	$30.00	$270.00
Swagelok SS-4-UT-6 1/4" union, Ultra-Torr Vacuum Fitting	3	$40.00	$120.00
Miscellaneous (*e.g.*, nuts, ferrules, unions)	1	$200.00	$200.00
1/4" stainless steel tubing (per foot)	17	$20.00	$340.00
AVS clamshell furnace	1	$1,900.00	$1,900.00
80/20 support stand	1	$700.00	$700.00
PP Systems WMA-4 CO2 analyzer	1	$2,100.00	$2,100.00
Metal Bellow MB-21 pump	1	$1,200.00	$1,200.00
Omega thermocouple, type K	2	$30.00	$60.00
Omega pressure gauge	1	$20.00	$20.00
Multi-tube (2) gas proportioning rotameter	1	$480.00	$480.00
50 mm rotameter	1	$120.00	$120.00
Glass reactor	1	$110.00	$110.00
Omega CN2110 series temperature controller	1	$400.00	$400.00
Cole-Parmer thermocouple temperature controller, type K and J, 110V	1	$80.00	$80.00
Total Estimated Cost			$8,920.00
* Prices as of December 2014			

A complete itemized parts list for the reaction unit with estimated costs is shown in Table 2. It is constructed as a modular unit that rests on a laboratory benchtop and only requires two gas feed lines, one exhaust line, and one electrical connection. The catalytic reactor is constructed out of borosilicate glass and consists of a preheating coil, a catalyst section, and a

U-shaped effluent line (Figure 2). The catalyst section contains a thermowell for a K-type thermocouple, which is used for temperature indication that is displayed on a readout, and a catalyst bed, which is supported by a porous glass frit. An O-ring with a Swagelok™ Ultra-Torr vacuum fitting seals the thermowell from the catalyst section.

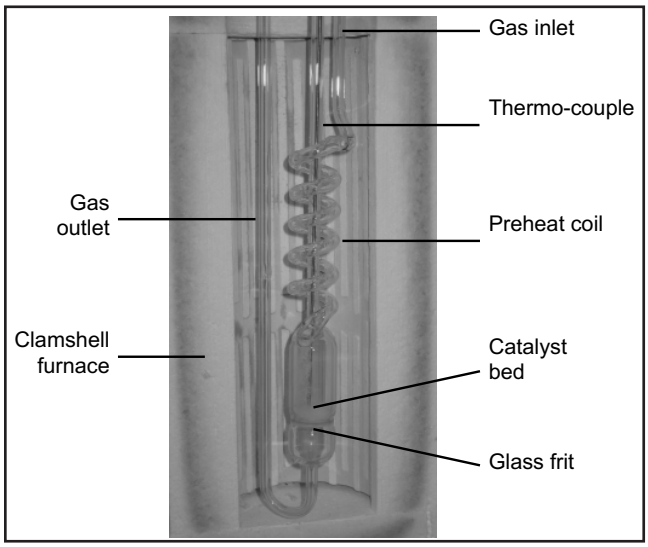

Figure 2. *The cross-section view of the clamshell furnace showing the glass reactor with K-type thermocouple inserted into catalyst bed, which is supported by a glass frit.*

Prior to the start of the experiments, 0.25 g of a 0.5 wt% Pd/Al_2O_3 catalyst powder is loaded into the reactor by pouring the catalyst through the thermowell and onto the glass frit. In order to study the effects of heat and mass transfer limitations on the reaction rate in subsequent experiments, the powder catalyst can be replaced with Pd/Al_2O_3 pellets of a desired size. The reactor is heated by using a clamshell furnace, which contains a thermocouple connected to a temperature controller.

As shown in Figure 3, the catalytic reaction unit can simulate three different ideal reactor configurations: batch, plug-flow (PFR), and continuous stirred-tank (CSTR). The flow paths for each mode of operation are indicated by the thick lines in Figure 3. The batch and CSTR configurations incorporate a metal bellows recirculation pump, which recycles product gases to the reactor feed at high enough flow rates to simulate well-mixed behavior.[6,11] The PFR configuration is a single-pass mode of operation. Gas delivery flow rates are measured and controlled by two rotameters with integral needle valves: one rotameter for the methane/air mixture, and the other for the nitrogen diluent to adjust the methane/air concentration. A CO_2 analyzer collects a slip-stream of the effluent gas mixture and analyzes the CO_2 concentration by using a non-destructive infrared (IR)-based sensor, and then returns the gas to the process stream.

The students measure the instantaneous CO_2 concentration at the reactor outlet by using the analyzer, and then average CO_2 readings over a time interval to minimize the error introduced from instrument noise. The exit CO_2 concentration

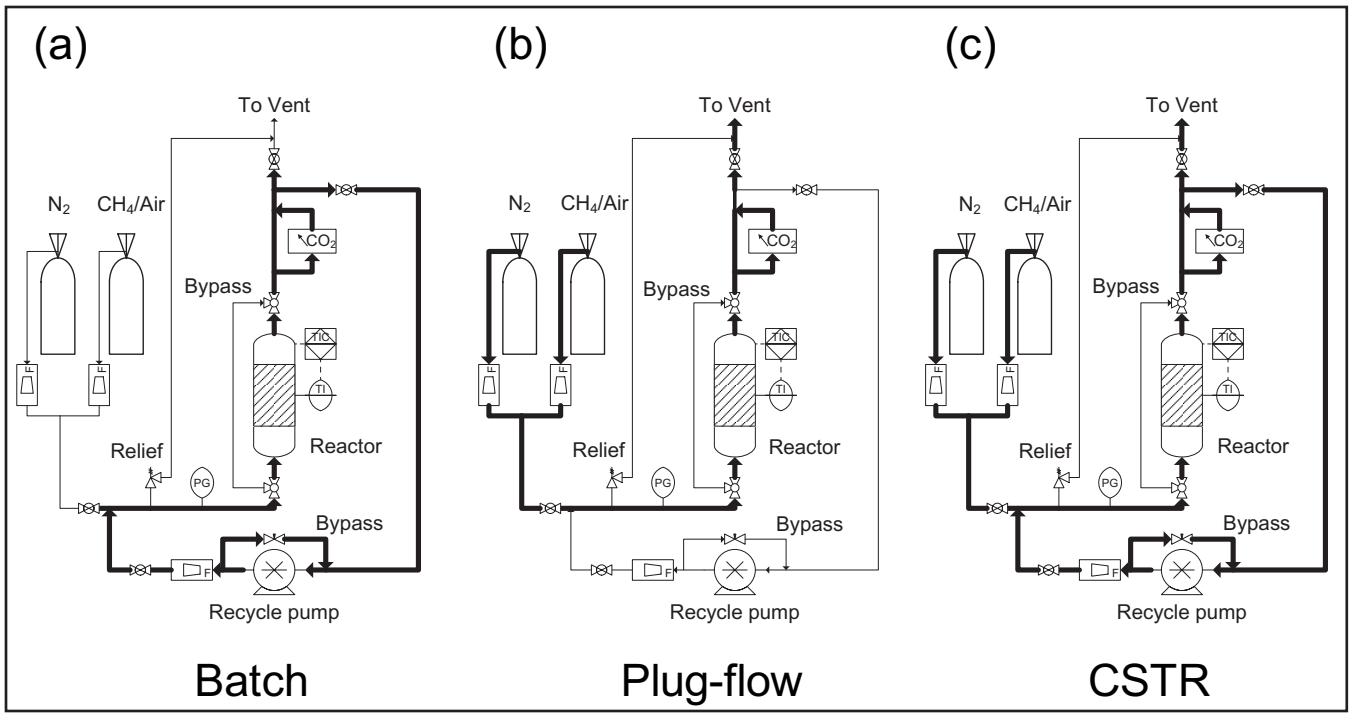

Figure 3. *Process flow schematic showing the different ideal reactor configurations for the experimental setup: (a) batch, (b) plug-flow (PFR), and (c) continuous stirred-tank (CSTR). Flow paths for each configuration are designated by thick dark lines.*

and inlet methane concentration are used to calculate the methane conversion at the exit of the catalyst bed (see "Calculations" section). During the experiments, the flow rates of the methane/air mixture and of nitrogen, along with the reactor temperature, can be adjusted to achieve a desired methane conversion (4 – 6%, within the differential limit of <10%).

In experiments to determine the activation energy, the reactor temperature is varied across a 40 – 50 K temperature range while the methane/air mixture and nitrogen flow rates are held constant. In experiments to determine the apparent reaction order for methane, the methane feed concentration is varied while the total flow rate and reaction temperature are held constant. The methane concentration is varied by adjusting the flow rates of the methane/air mixture and the nitrogen diluent to maintain a constant total flow rate. Since oxygen is in excess, the order of reaction for oxygen is assumed to be zero,[10,12] which means that the change in air concentration has a negligible effect on the reaction rate.

SAFETY

The lower and upper explosive limits (LEL/UEL) for methane in air are 5 vol% and 15 vol%,[13] respectively. In these experiments, we use pre-mixed methane/air mixtures containing 1 – 2.5 vol% methane to guarantee that the operating range will always remain outside of the explosion region. Another benefit of using these methane/air mixtures is to ensure that O_2 will remain in excess (~4X molar excess) of the stoichiometric amount required for complete oxidation of methane, thus avoiding CO formation from partial oxidation ($CH_4 + 3/2O_2 \rightarrow CO + 2H_2O$). The presence of CO in the reactor would require additional laboratory safety devices, including an atmospheric CO gas detector connected to an automated safety shut-off valve to stop the methane/air flow to the reactor in the event of a leak. The proposed laboratory experiments are designed specifically to eliminate hazards associated with CO exposure. The reactor exhaust in the current apparatus is connected to a ventilated fume hood in order to prevent exposure to the laboratory.

Additional safety features include a pressure relief valve, set to 5 psig, that is installed upstream of the reactor for protection in the unlikely event of overpressure. The reactor by-pass can be used at any time to stop the reaction. Safety glasses must be worn at all times during operation of the laboratory reactor unit and users should exercise caution to avoid contact with the furnace and external tubing to prevent thermal burns.

CALCULATIONS

The methane conversion is determined by the number of moles of methane that have reacted per mole of methane fed to the system, which can be determined for flow reactors from the measured outlet concentration of CO_2 (1 mole of CO_2 is formed per mole of CH_4 reacted) and the known inlet concentration of methane:

$$X = \frac{qC_{CO_2}}{q_0 C_{CH_{4,0}}} = \frac{C_{CO_2}}{C_{CH_{4,0}}} \text{ when } q = q_0 \quad (1)$$

In Eq. (1), X is the conversion of methane, q_0 is the inlet volumetric flow rate (liters s^{-1}), q is the outlet volumetric flow rate (liters s^{-1}), C_i is the concentration of species i (moles $liter^{-1}$) and $C_{i,0}$ is the concentration of species i at the inlet (moles $liter^{-1}$). Since CO_2 and water are the only products of the reaction ($CH_4 + 2O_2 \rightarrow CO_2 + 2H_2O$), the total number of moles is conserved during the reaction and the inlet and outlet flow rates are equal.

The relation between the reaction rate and the measured parameters is derived from the mole balance on the species of interest for a particular system. For the batch reactor, the rate is given by:

$$r = \frac{V}{W}\frac{dC_{CO_2}}{dt} \quad (2)$$

where r is the rate [(mole CO_2) (g_{cat}^{-1}) s^{-1}]; V is the reactor volume (liters); W is the mass of catalyst (grams of catalyst); and C_{CO_2} is the concentration of CO_2 (moles $liter^{-1}$).

The CSTR rate equation is given by:

$$r = \frac{qC_{CO_2}}{W} \quad (3)$$

where r is the rate [(mole CO_2) (g_{cat}^{-1}) s^{-1}]; q is the volumetric flow rate (liters s^{-1}); W is the mass of catalyst (grams); and C_{CO_2} is the concentration of CO_2 (moles $liter^{-1}$).

The differential form of the PFR rate expression is:

$$r = qC_{CH_{4,0}}\frac{dX}{dW} \quad (4)$$

In the limit of low conversion ($X < 0.1$), the concentrations and temperature are often assumed to be constant throughout the reactor, in which case the integration of Eq. (4) yields Eq. (3). If the PFR cannot be considered differential, however, then the reaction rate can be calculated from the PFR data if the dependence of rates with concentration is known [Eq. (5)].

In order to measure the temperature and concentration dependences of the rate, the experimental data are fitted to a power law expression:

$$r = k_{app} C_{CH_4}^{\alpha} C_{O_2}^{\beta} C_{CO_2}^{\gamma} C_{H_2O}^{\delta} \quad (5)$$

$$k_{app} = A \exp\left(\frac{-E_{app}}{RT}\right) \quad (6)$$

where k_{app} is the apparent rate constant; α, β, γ, and δ are the apparent reaction orders with respect to concentrations of CH_4, O_2, CO_2, and H_2O, respectively; A is the pre-exponential factor; E_{app} is the apparent activation energy (kJ $mole^{-1}$); R is the universal gas constant (kJ $mole^{-1}$ K^{-1}); and T is the reaction temperature (K).

By combining Eqs. (5) and (6), the overall power law rate expression is given as:

$$r = A\exp\left(\frac{-E_{app}}{RT}\right)C_{CH_4}^{\alpha}C_{O_2}^{\beta}C_{CO_2}^{\gamma}C_{H_2O}^{\delta} \qquad (7)$$

Taking the natural log of both sides of the power law rate expression [Eq. (7)] gives:

$$\ln(r) = \ln\left(AC_{CH_4}^{\alpha}C_{O_2}^{\beta}C_{CO_2}^{\gamma}C_{H_2O}^{\delta}\right) - \frac{E_{app}}{R}\left(\frac{1}{T}\right) \qquad (8)$$

A plot of ln(r) versus T^{-1} [Eq. (8)] allows the calculation of the apparent activation energy from the slope of $-E_{app}/R$, if the experiments are performed with constant reactant and product concentrations.

Additionally, the apparent reaction order for methane can be determined from the power law rate expression in Eq. (5) when the data are collected at a fixed temperature. We assume that the orders for O_2 and CO_2 are zero because oxygen is in excess and because there is no inhibition of the reaction rate by CO_2 (below 0.5% CO_2).[10,12] If inhibition by H_2O is also ignored, then the H_2O order is assumed to be zero[10,12,14] and the rate expression reduces to:

$$r = k_{app}C_{CH_4}^{\alpha} = k_{app}\left[C_{CH_4,0}^{\alpha}(1-X)\right]^{\alpha} = k_{app}C_{CH_4,0}^{\alpha}, \text{ for } 1-X \approx 1 \qquad (9)$$

From the linear regression of ln(r) versus ln($C_{CH_4,0}$), the apparent order of reaction for methane, α_{app}, is given by the slope.

Researchers have shown, however, that the oxidation of methane on supported Pd catalysts is inhibited by H_2O,[10,12,14] a product of the methane oxidation reaction. By using the experimentally determined H_2O reaction order of -1, the rate expression in Eq. (5) becomes:

$$r = k_{app}\frac{C_{CH_4}^{\alpha}}{C_{H_2O}} = k_{app}\frac{\left[C_{CH_4,0}(1-X)\right]^{\alpha}}{2C_{CH_4,0}X} \approx \frac{k_{app}C_{CH_4,0}^{\alpha-1}}{2X} \text{ for } 1-X \approx 1 \qquad (10)$$

Proper accounting of the effects of product inhibition on the reaction kinetics can be accomplished by using a straightforward mathematical treatment of the experimental data. However, the instructor can choose to simplify the mathematical analysis for the students by assuming that the methane oxidation rate is uninhibited by the reaction products. Under this assumption, the reaction rates, apparent activation energies, and apparent methane order can be determined more simply. The simplified analysis provides students with a qualitative understanding of the effects of operating parameters, such as reactant partial pressure, temperature, and catalyst particle size, on the methane oxidation rate. The implications of the important differences between these two methods of data analysis (with and without water inhibition) are discussed below.

RESULTS

Methane oxidation kinetics with water inhibition

The order of reaction for methane in the CSTR configuration, accounting for H_2O inhibition of the reaction rate, is determined by substituting the rate expression from Eq. (10) into Eq. (3) and rearranging to solve for X as follows:

$$\frac{qC_{CH_4,0}X}{W} = \frac{C_{CH_4,0}X}{\tau} = \frac{k_{app}C_{CH_4,0}^{\alpha-1}}{2X}, \text{ for } \tau = \frac{W}{q} \qquad (11)$$

$$X = \left(\frac{\tau k_{app}C_{CH_4,0}^{\alpha-2}}{2}\right)^{1/2} \qquad (12)$$

By combining Eqs. (12) and (10), the simplified rate expression becomes:

$$r = \frac{k_{app}C_{CH_4,0}^{\alpha-1}}{2X} = \frac{k_{app}C_{CH_4,0}^{\alpha-1}}{2\left(\frac{\tau k_{app}C_{CH_4,0}^{\alpha-2}}{2}\right)^{1/2}} = \left(\frac{k_{app}}{2\tau}\right)^{1/2}C_{CH_4,0}^{\alpha/2} \qquad (13)$$

The slope of the linear regression of ln(r) versus ln($C_{CH_4,0}$) gives the apparent reaction order for methane, α_{app}. Eq. (13), however, shows that the true reaction order for methane (α) is related to the apparent reaction order (α_{app}) by $\alpha = 2\alpha_{app}$. Thus, the true methane reaction order for the CSTR is 1.0±0.2. Similarly, for the batch and PFR configurations, the methane reaction orders are 1.1±0.2 and 0.8±0.2, respectively, as shown in Table 3. These values are in agreement with the methane reaction

TABLE 3
Methane oxidation kinetics for various reactors on a 0.5 wt% Pd/Al_2O_3 powder catalyst with water inhibition

Reactor	Rate [a] /10^{-7} (mole CO_2) (g_{cat}^{-1}) s^{-1}	α [b]	E^{*} [c] /kJ $mole^{-1}$	E_{app} /kJ $mole^{-1}$
Batch [d]	1.5±0.2	1.1±0.2	85±5	169±9
Plug-flow [e]	1.3±0.2	0.8±0.2	88±3	176±6
CSTR	1.6±0.1	1.0±0.2	91±1	181±2

a Rates determined at 506 K with 1.2% CH_4, 9.7% O_2, 0.1% H_2O, and balance N_2 at 0.13 liter min^{-1} total flow.
b CH_4 reaction order was measured at 506 K by assuming reaction orders of -1 for H_2O, and 0 for O_2 and CO_2.
c Measured between 498 – 528 K.
d Batch rates are determined from initial reaction rates [Eq. (2)] measured with 1.2% CH_4, 9.7% O_2, 0.1% H_2O, and balance N_2.
e PFR rates determined according to PFR model [Eq. (16)] and the power law rate expression [Eq. (10)] with 1.2% CH_4, 9.7% O_2, 0.1% H_2O, and balance N_2.

order of 1.1±0.1 measured by Fujimoto, et al.[12] on Pd/ZrO_2.

The apparent activation energy is determined from Eq. (8) by plotting ln(r) as a function of T^{-1} for a fixed initial concentration of methane. Eq. (13) shows that the measured rate, accounting for H_2O inhibition [Eq. (10)], is proportional to $k^{1/2}$ for the CSTR configuration. Thus, the overall power law rate expression is:

$$r = \left(\frac{k}{2\tau}\right)^{1/2} C_{CH_{4,0}}^{\alpha/2} = \left(\frac{A}{2\tau}\right)^{1/2} \exp\left(\frac{-E_{app}}{2RT}\right) C_{CH_{4,0}}^{\alpha/2} \qquad (14)$$

Taking the natural log of both sides of Eq. (14) gives:

$$\ln(r) = \frac{1}{2}\ln\left(\frac{AC_{CH_{4,0}}}{2\tau}\right) - \frac{E_{app}}{2R}\left(\frac{1}{T}\right) \text{ for } \alpha = 1 \qquad (15)$$

A comparison of the temperature dependent terms in Eqs. (15) and (8) shows that the apparent activation energy (E_{app}) for methane oxidation is related to the slope of ln(r) versus T^{-1}, denoted as E^*, by $E_{app} = 2E^*$. Thus, the apparent activation energy measured in the CSTR configuration is 181±2 kJ $mole^{-1}$ (Table 3).

The kinetics in the PFR configuration, accounting for H_2O inhibition, were determined by using the differential form of the PFR model [Eq. (4)] with actual reaction orders. The following expression for the apparent rate constant can be derived by using Eq. (4) and the rate law with the correct H_2O order of -1 (full derivation provided in the supplemental information available online):

$$k_{app} = \frac{C_{CH_{4,0}}}{\tau} X^2 \qquad (16)$$

The apparent activation energy determined by the slope of $\ln(k_{app})$ versus T^{-1} from the PFR model that accounts for H_2O inhibition [Eq. (16)] is 176±6 kJ $mole^{-1}$ (Table 3). This apparent activation energy is twice the value of 88±3 kJ $mole^{-1}$ for E^*, which is determined by the slope of ln(r) versus T^{-1} and does not account for H_2O inhibition. The methane oxidation rate for the PFR (Table 3) with H_2O inhibition, calculated by using the power law rate expression [Eq. (10)] and k_{app} from the PFR model [Eq. (16)], is 1.3×10^{-7} (mole CO_2) (g_{cat}^{-1}) s^{-1} at 506 K (1.2% CH_4, 9.7% O_2, 0.1% H_2O, and balance N_2) and is within 15% of the rates calculated for the batch and CSTR configurations.

A similar correction for H_2O inhibition is applied to the batch reactor to show that the apparent activation energy for the batch configuration is 169±9 kJ $mole^{-1}$, which agrees with the values determined in the PFR and CSTR modes. The batch reactor rates are reported as initial rates where the H_2O concentration (0.1% H_2O) is similar to that within the CSTR.

Simplified methane oxidation kinetics by assuming no water inhibition

If the methane oxidation reaction is assumed to be zero order in H_2O and that differential conditions can be achieved, then the reaction rate for the PFR, like the CSTR, can be determined directly from the experimental data according to Eq. (3). Based on this assumption, the rate for the PFR at an average methane conversion of 4.9% is shown in Table 4 along with rates for batch and CSTR configurations at average methane conversions of 4.5% and 4.3%, respectively, at 506 K (1.2% CH_4, 9.7% O_2, 0.1% H_2O, and balance N_2). Reaction rates for the batch and CSTR were identical within experimental error, but lower than rates for the PFR (Table 3). The reason for this rate discrepancy is because H_2O inhibits[10,14] the methane oxidation reaction by competing with methane for Pd surface sites. The PFR contains no water at the inlet of the catalyst bed, while the CSTR (with a recycled product stream) and batch reactor (started from the CSTR configuration at steady state) contain a finite concentration of H_2O at initial times. These results demonstrate that the PFR cannot be considered a differential reactor when reaction products inhibit the reaction rate, even though the PFR is often modeled as a CSTR in the limit of low conversion out of convenience to directly calculate the rate from an algebraic equation [Eq. (3)].

Fortunately, there is a straightforward experimental solution that removes complications in the kinetic analysis caused by product inhibition in the PFR. Addition of water to the reactor feed, in an amount that results in only a differential change (<10% of its initial value) in water concentration along the length of the bed due to the chemical reaction, ensures that the

TABLE 4
Methane oxidation kinetic parameters for different ideal reactor types on a 0.5 wt% Pd/Al_2O_3 powder catalyst from analysis that assumes no water inhibition

Reactor	Rate [a] / 10^{-7} (mole CO_2) (g_{cat}^{-1}) s^{-1}	α_{app} [b]	E^* [c] / kJ $mole^{-1}$
Batch [d]	1.5±0.2	0.6±0.1	85±5
Plug-flow [e]	2.2±0.2	0.4±0.1	88±3
CSTR	1.6±0.1	0.5±0.1	91±1

a Rates determined at 506 K with 1.2% CH_4, 9.7% O_2, 0.1% H_2O, and balance N_2 at 0.13 liter min^{-1} total flow.
b CH_4 reaction order measured at 506 K, by assuming reaction orders of 0 for H_2O, O_2, and CO_2.
c Measured between 498 – 528 K.
d Batch rates are determined from initial reaction rates [Eq. (2)] measured with 1.2% CH_4, 9.7% O_2, 0.1% H_2O, and balance N_2.
e PFR rates determined according to the CSTR model for differential reactor [Eq. (3)] without accounting for water inhibition.

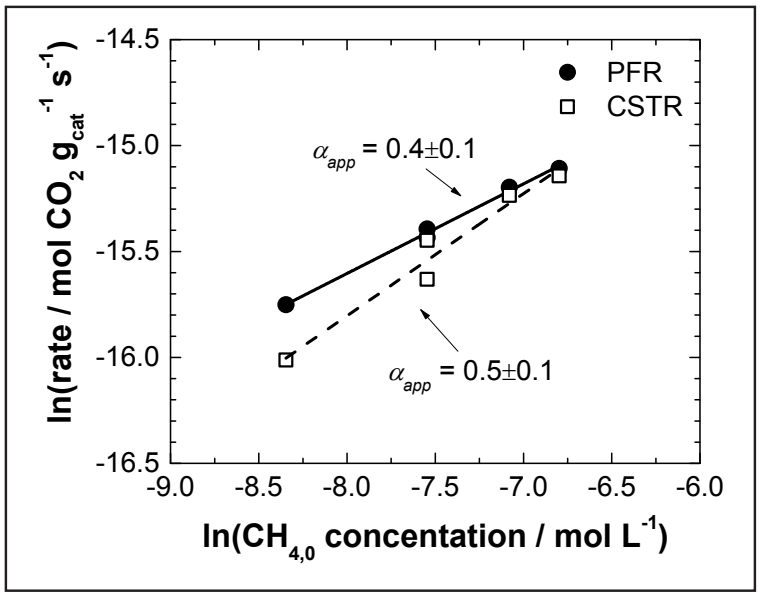

Figure 4. *Apparent methane reaction orders obtained from rates determined by using the CSTR model [Eq. (3)] at 506 K on 0.5 wt.% Pd/Al_2O_3 in the PFR (circles) and CSTR (squares), neglecting inhibition by H_2O.*

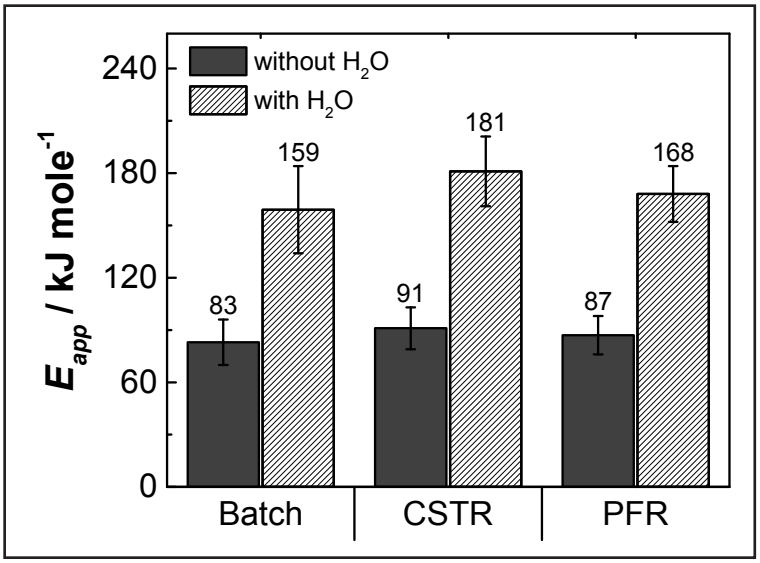

Figure 5. *Activation energy comparison of the averaged student data for the three reactor configurations without inhibition by H_2O (solid) and with inhibition by H_2O (shaded). Error bars are determined based on the standard deviation according to the "n-1" method.*

rate is approximately constant throughout the reactor and that the PFR operates as a differential reactor and can be modeled as a CSTR (Eq. (3)). The capability of co-feeding products, however, has not been added to the reactor setup described in this experiment (Figure 1). It can be easily done by adding a water saturator to the feed.

Our instructional reactor unit is mobile, is constructed with inherent safety features, and is versatile in its ability to perform multiple types of experiments with precise measurements.

The experimentally determined rates in Table 4, ranging from 1.5 to 2.2 × 10^{-7} (mole CO_2) (g_{cat}^{-1}) s^{-1} at 506 K (1.2% CH_4, 9.7% O_2, 0.1% H_2O, and balance N_2), are comparable to those obtained by Ribeiro, et al.[10] for methane oxidation on supported Pd catalysts (0.9 to 5 × 10^{-7} (mole CO_2) (g_{cat}^{-1}) s^{-1} extrapolated to 506 K with 1.2% CH_4, 9.7% O_2, 0.1% H_2O and E_{app} = 82 kJ $mole^{-1}$). The apparent reaction orders for methane on the 0.5 wt% Pd/Al_2O_3 powder catalyst in the PFR and CSTR configurations were determined from the data in Figure 4 to be 0.4±0.1 and 0.5±0.1, respectively (Table 4). Similarly, the apparent reaction order for methane in the batch reactor was determined to be 0.6±0.1. The slopes of ln(r) versus T^{-1} (E^*) for the three reactors were also similar, ranging from 85 to 91 kJ mol^{-1}. We reiterate that these apparent methane reaction orders and activation energies (Table 4) were estimated by using rate equations that assume the H_2O reaction order is zero and result in falsified kinetic values. These falsified kinetic values (Table 4) have instructive value when compared to the true kinetic values (Table 3), because it illustrates the corruption of kinetic measurements due to product inhibition.

Student laboratory results

Apparent activation energies and methane reaction orders obtained by using the three reactors (batch, CSTR, PFR) for the methane catalytic oxidation experiment were collected from eight groups of chemical engineering students (29 total students) at Purdue University. Figure 5 shows a comparison of the activation energies determined by the students for each reactor, both with and without accounting for the effect of water inhibition on the reaction rate. The reported values are averages of the data obtained by the eight student groups. When water inhibition is neglected, the students measured E^* values of 83±13, 91±12, and 87±11 kJ $mole^{-1}$ for the batch, CSTR, and PFR configurations, respectively. Taking into account the inhibition of water on the reaction rate, the apparent activation energies reported are 159±25, 181±20, and 168±16 kJ $mole^{-1}$ for the batch, CSTR, and PFR configurations, respectively. These values are in reasonable agreement with those listed in Table 3.

The average values of the methane reaction order for the three reactor types are shown in Figure 6. For the case without inhibition by water, the apparent methane reaction orders measured in each reactor are 0.6±0.1. When water inhibition is included in the analysis, the methane reaction orders are 0.9±0.3 for the batch reactor, and 1.0±0.2 for both the CSTR and PFR. These results are in excellent agreement with those reported in Table 3, as well as in the literature.[12,15]

In order to examine the effect of internal mass transfer resistance on the reaction rate, the students replaced the powder 0.5 wt% Pd/Al_2O_3 catalyst with cylindrical pellets (3.3 mm L x 3.5 mm D) of 0.5 wt% Pd/Al_2O_3, and then determined the apparent activation energy from the PFR configuration. Figure 7 shows an Arrhenius plot of $\ln(k_{app})$ versus T^{-1}, in which the apparent activation energies for the two different catalyst particle sizes are compared by using the PFR model with H_2O inhibition to extract k_{app} [Eq. (16)]. The apparent activation energy of 176±6 kJ $mole^{-1}$ for the 0.5 wt% Pd/Al_2O_3 catalyst powder is approximately twice that of the 0.5 wt% Pd/Al_2O_3 pellet (91±1 kJ $mole^{-1}$), which indicates that internal diffusion limitations are present.[16] This exercise allows the students to observe how kinetics can also be falsified in the presence of mass transfer resistance, which can have important consequences in fundamental studies of chemical kinetics and in industrial applications for reactor design. For example, if the particle size of the catalyst pellet were reduced, the higher apparent activation energy would cause the reaction rate to become more sensitive to temperature and potentially increase the probability of a runaway reaction.[16]

CONCLUSIONS

By properly accounting for inhibition of the reaction rate by H_2O, students can measure apparent methane reaction orders, reaction rates, and apparent activation energies on a supported 0.5 wt% Pd/Al_2O_3 catalyst that are similar for the three types of ideal reactors and that are in agreement with results published in the literature for supported Pd catalysts. From these experiments, students observe that the reactor configurations incorporating product recycle (CSTR, batch) exhibit lower rates than the single-pass PFR configuration under the same reaction conditions, because one of the reaction products (H_2O) inhibits the reaction rate. In this case, the PFR cannot be considered a differential reactor, since the reaction rate varies with conversion and H_2O pressure along the length of the reactor.

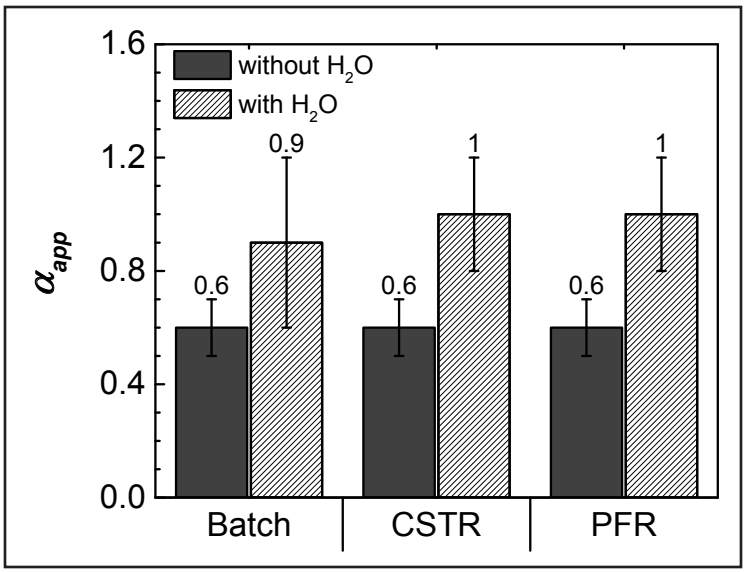

Figure 6. *Methane reaction order comparison of the averaged student data for the three reactor configurations without inhibition by H_2O (solid) and with inhibition by H_2O (shaded). Error bars are determined based on the standard deviation according to the "n-1" method.*

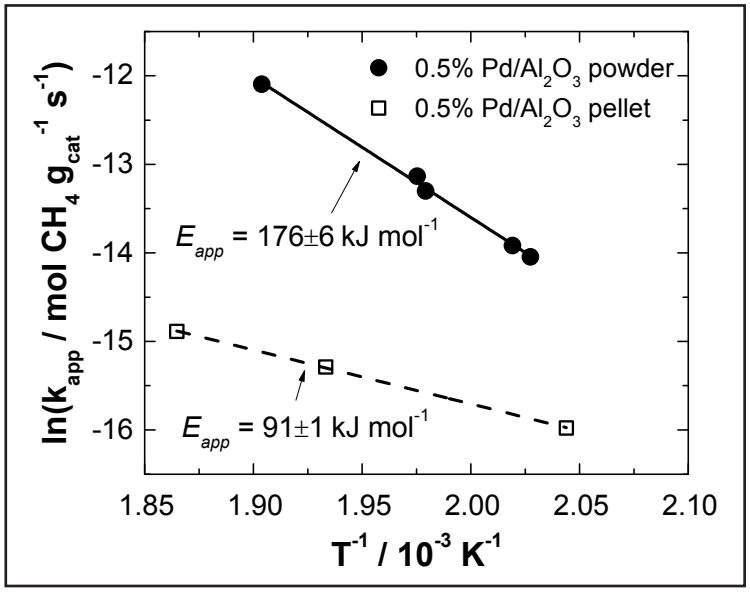

Figure 7. *Arrhenius plots comparing the effect of internal mass transfer resistance for 0.5 wt.% Pd/Al_2O_3 powder (circles) versus 0.5 wt.% Pd/Al_2O_3 pellets (squares). Apparent rate constants for the PFR were determined from measurements between 498 – 528 K (1.2% CH_4, 9.7% O_2, 0.1% H_2O, and balance N_2) by using Eq. (16) to account for water inhibition.*

An important lesson demonstrated by the experiments in our instructional reactor unit is that falsified kinetics can be measured when the products of a reaction inhibit the reaction rate. In these instances, the measured apparent activation energies and reaction orders are different from their true values. In lieu of co-feeding the products with the

reactants to assure their concentrations, and the reaction rate in turn, are constant throughout the reactor at low conversion, proper treatment of the experimental data that explicitly accounts for product inhibition is necessary to accurately estimate kinetic parameters and apply them to solve reaction engineering problems.

Additionally, by comparing apparent activation energies for 0.5 wt% Pd/Al_2O_3 catalysts of different particle sizes, students learn that internal mass transfer resistance within catalyst pellets can also lead to falsified kinetics. When intrapellet concentrations differ from external fluid concentrations, the reaction rate is no longer solely dependent on the number of catalytic sites in the pellet, but instead becomes limited by the internal diffusion of reactants to the active sites.

These findings show that chemical engineering students can use this versatile laboratory reactor unit successfully as a hands-on tool to learn important concepts in chemical kinetics, catalysis, and reaction engineering on a system with real-world applications.

SUPPLEMENTAL INFORMATION

Additional figures of the glass reactor and laboratory unit, derivation of the PFR model with water inhibition, and instructional materials are available via the internet at <https://engineering.purdue.edu/~catalyst/publications.html>.

ACKNOWLEDGMENTS

This laboratory activity was made possible through the generous financial support of BP, Dow Chemical Company, LyondellBasell Industries, Procter & Gamble, Roquette America, Inc., and Shell.

REFERENCES

1. Varma, A. and I.E. Grossmann, "Evolving Trends in Chemical Engineering Education," *AIChE J*., **11**, 3692 (2014)
2. Heveling, J., "Heterogeneous Catalytic Chemistry by Example of Industrial Applications," *J. Chem. Ed*., **89**, 1530 (2012)
3. Boudart, M., and G. Djega-Mariadassou, *Kinetics of Heterogeneous Catalytic Reactions*, Princeton University Press, Princeton, NJ (1984)
4. Andres, R.P. and L.R. Hile, "Alkaline Fading of Organic Dyes: An Ideal Reaction for Homogeneous Reactor Experiments," *Chem. Eng. Ed.,* **10**(1), 18 (1976)
5. Mendes, A.M., L.M. Madeira, F.D. Magalhes, and J.M. Sousa, "An Integrated Chemical Reaction Engineering Lab Experiment," *Chem. Eng. Ed*., **38**(3), 228 (2004)
6. Paspek, S.C., A. Varma, and J.J. Carberry, "Utilization of the Recycle Reactor in Determining Kinetics of Gas-Solid Catalytic Reactions," *Chem. Eng. Ed*., **14**(2), 78 (1980)
7. Saddawi, S., and Schmitz, R.A., "Experiments with a Fixed-Bed Catalytic Reactor," *Chem. Eng. Ed*., **36**(1), 34 (2002)
8. Pfefferle, L.D. and W.C. Pfefferle, "Catalysis in Combustion," *Catal. Rev.-Sci. Eng*., **2**, 219 (1987)
9. Anderson, R.B., K.C. Stein, J.J. Feenan, and L.J.E. Hofer, "Catalytic Oxidation of Methane," *Ind. Eng. Chem*., **53**, 809 (1961)
10. Ribeiro, F.H., M. Chow, and R.A. Dallabetta, "Kinetics of the Complete Oxidation of Methane over Supported Palladium Catalysts," *J. Catal*., **2**, 537 (1994)
11. Hill, C.G., and T.W. Root, *Introduction to Chemical Engineering Kinetics and Reactor Design*, Wiley, Hoboken, NJ (2014)
12. Fujimoto, K.-I., F.H. Ribeiro, M. Avalos-Borja, and E. Iglesia, "Structure and Reactivity of PdO_x/ZrO_2Catalysts for Methane Oxidation at Low Temperatures," *J. Catal*., **2**, 431 (1998)
13. GPSA, *Engineering Data Book*, Gas Processors Supliers Association, Tulsa, OK (2004)
14. Ciuparu, D., M.R. Lyubovsky, E. Altman, L.D. Pfefferle, and A. Datye, "Catalytic Combustion of Methane Over Palladium-Based Catalysts," *Catal. Rev.- Sci. Eng*., **4**, 593 (2002)
15. Monteiro, R.S., D. Zemlyanov, J.M. Storey, and F.H. Ribeiro, "Surface Area Increase on Pd Foils After Oxidation in Excess Methane," *J. Catal*., **1**, 37 (2001)
16. Fogler, H.S., *Elements of Chemical Reaction Engineering*, Pearson Education, Inc., Boston, MA (2006) ❐